

Cellular V2X Communications in the Presence of Big Vehicle Shadowing: Performance Analysis and Mitigation

Hieu T. Nguyen , Md. Noor-A-Rahim , Yong Liang Guan , *Senior Member, IEEE*,
and Dirk Pesch , *Senior Member, IEEE*

Abstract—In Intelligent Transportation Systems (ITS), vehicular networks are enabling technologies for onboard data services such as traffic safety, user infotainment, etc. Vehicular networks face many challenges when it comes to providing satisfactory quality of service, mainly because of issues that arise from unreliable communication in unfavorable propagation conditions. One prime example is Vehicle-to-Vehicle (V2V) communication in the presence of big vehicles that present obstacles in the communication path of smaller vehicles, where the signal strength decays drastically due to the big vehicle shadowing. As a result, the communication range is shortened, and the safety message dissemination capability is reduced. In this paper, we analyze the impact of big vehicle shadowing on V2V communications, taking into account Cellular Vehicle-to-Everything (C-V2X) networks. A geometric as well as a stochastic approach is employed to analyze the length of shadow regions for conventional cars and big vehicles on the road in different scenarios. This paper analyses the effect of large vehicles shadowing on a V2V communication link as a function of the shadow region length. A beamforming-based signal reception technique is proposed in order to mitigate packet collisions caused by hidden nodes. Considering relaying operation by big vehicles, three relaying schemes are proposed to improve the V2V message dissemination performance. Extensive simulations are conducted to demonstrate the effectiveness of the proposed schemes.

Index Terms—C-V2X, LTE sidelink mode-4, 5G-NR sidelink mode-2a, autonomous mode, smart beamforming, V2V communications, relaying, cooperative V2X communications, big vehicle shadowing.

I. INTRODUCTION

VEHICLE-to-Vehicle (V2V) communication is seen as an essential tool for road safety, collision/accident avoidance,

Manuscript received 27 March 2022; revised 9 September 2022; accepted 25 September 2022. Date of publication 10 October 2022; date of current version 14 March 2023. The work of Yong Liang Guan and Hieu T. Nguyen was supported by A*STAR, Singapore through the RIE2020 Advanced Manufacturing and Engineering (AME) Industry Alignment Fund-Pre Positioning (IAF-PP) under Grant A19D6a0053. The work of Md. Noor-A-Rahim and Dirk Pesch was supported by Science Foundation Ireland through CONNECT: The Centre for Future Networks and Communications under Grant 13/RC/2077_P2 and through Enable Spoke Programme under Grant 16/SP/3804. The review of this article was coordinated by Prof. Jun Zheng. (*Corresponding author: Md. Noor-A-Rahim.*)

Hieu T. Nguyen and Yong Liang Guan are with the School of Electrical and Electronic Engineering (EEE), Nanyang Technological University (NTU), Singapore 639798 (e-mail: nguyenth@ntu.edu.sg; eylguan@ntu.edu.sg).

Md. Noor-A-Rahim and Dirk Pesch are with the School of Computer Science and IT, University College Cork, T12 K8AF Cork, Ireland (e-mail: m.rahim@cs.ucc.ie; d.pesch@cs.ucc.ie).

Digital Object Identifier 10.1109/TVT.2022.3212704

and autonomous driving in Intelligent Transportation Systems (ITS). In V2V communication, vehicles communicate with one another via safety message exchanges to alert each other of dangerous situations or accidents, and improve traffic conditions. A safety message contains information about a vehicle's instantaneous manoeuvres (such as location, speed, acceleration, heading, etc.) and other aspects such as the type of vehicle and brake conditions. For enhanced driver safety and comfort, a suitable audio/visual warning is displayed based on the received safety information from neighboring vehicles. Each year, the United States has more than thirty thousand fatal crashes involving vehicles, according to the National Highway Traffic Safety Administration (NHTSA). Research indicates that the successful deployment of vehicular networks could reduce 82% of these accidents [1]. Thus, it is crucial to implement reliable V2V communication with sufficient radio coverage to avoid accidents and collisions.

At present, there are two main technologies used for vehicular communications, (i) the DSRC (Dedicated Short Range Communication)-based vehicular network and (ii) a cellular-based vehicular network (C-V2X). A number of standards serve as the basis for DSRC including IEEE 802.11p for Wireless Access in Vehicular Environments (WAVE), IEEE 1609.1.4 for resource management, security, network service, and multi-channel operation. Meanwhile, cellular vehicular communication, also known as C-V2X, is developed by 3GPP for use in cellular networks, such as Long-Term Evolution (LTE) and 5 G New Radio (5 G NR). C-V2X technology enables vehicles to communicate while in coverage as well as while out of coverage of base stations. In the first scenario, the base station (i.e., eNodeB in LTE and gNodeB in 5G-NR) manages and allocates radio resources to its associated vehicles. A vehicle that is out of coverage, on the other hand, does not get base station support and allocates resources in a decentralized or autonomous fashion (e.g., LTE sidelink mode-4 [2] or 5G-NR sidelink mode-2a [3]). This article focuses on the dissemination of the Basic Safety Message (BSM) for the latter scenario i.e., when the vehicles are out of base station coverage.

In V2V communications, the quality of the wireless link is critical to the delivery of safety messages. Large obstructions such as a truck or a bus can significantly affect the quality of the V2V communication link due to the low position of the antennas

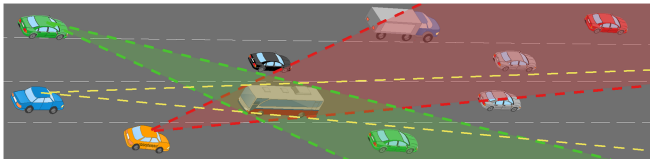


Fig. 1. Illustration of a highway with normal cars in shadows of big vehicles.

on the vehicle. Most of the existing V2V communications performance analyses have neglected to consider shadowing by big vehicles [4], [5], [6]. Several studies [7], [8] have shown that big vehicles can impede the line-of-sight (LOS) of V2V communications and significantly reduce the received signal strength. In a campus environment, the authors in [7] reported 15-20 dB loss in received signal strength caused by a single bus obstruction. According to another report [8], obstruction loss due to the big vehicle measures 8.6-10 dB. Multiple link shadowing was analyzed in [9] using measurement-based methods. A model for shadowing was proposed in [10], [11], [12], where aerial photography of a Portuguese highway near Porto was used to fit their model. This model was later used by authors in [13] to evaluate the performance of safety message broadcasting. An expression in semi-closed form was presented in [14] to show the blocking effect of a big vehicle at an intersection. More recently, authors in [15] analyzed the impact of the shadowing effect of big vehicles on DSRC-based V2V communication while taking into account both geometric and stochastic shadowing of multiple big vehicles. In terms of vehicular networks, all the above works either consider a generic network or a DSRC based network. To the best of our knowledge, no work has considered the impact of big vehicle shadowing on a C-V2X network. In addition, only a few studies (e.g., [16]) have investigated mitigation strategies to address the impact of big vehicles, ignoring real-world vehicular communication constraints (e.g., collisions of data packets).

Motivated by the above, we analyse in this paper the impact of big vehicle shadowing while considering a C-V2X network. The length of shadow region for each lane is analyzed based on both geometric and stochastic location for different scenarios of conventional cars and big vehicles on the road. The impact of big vehicle shadowing on the signal degradation of a V2V communication link is analysed as a function of the shadow region lengths. To mitigate packet collisions due to hidden nodes, a beamforming-based signal reception technique is proposed for all kinds of vehicles. Furthermore, we propose three relaying approaches via big vehicles namely, Front-Back relaying (FB-relaying), Network Coding¹ based on Geometric Shadowing relaying (NCG-relaying), and Lane-Selective Hierarchical relaying (H-relaying). The effectiveness of the proposed schemes is shown through extensive simulations.

The remainder of this article is organized as follows. Section II presents the system model and background on big vehicle shadowing. An analysis of the C-V2X autonomous mode is

¹Although network-coded relaying has been studied in the past (e.g. [17], [18]), existing works did not address the big-vehicle shadowing effects and did not utilize both the physical- and MAC-layer solutions as in this paper.

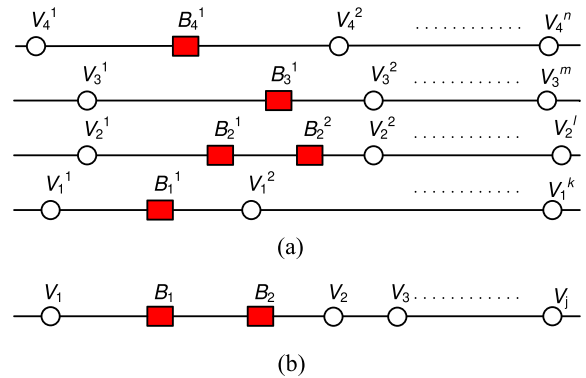


Fig. 2. (a) Normal and big vehicles on a 4-lane highway, and (b) Equivalent PPP model.

presented in Section III. A beamforming-based signal reception scheme is proposed in Section IV to tackle the hidden node problem. In Section V, three relaying schemes are proposed to mitigate the impact of big vehicle shadowing. Simulation results are presented in Section VI. Finally, the paper is concluded in Section VII.

II. SYSTEM MODEL, BIG VEHICLE SHADOWING AND PATH-LOSS MODELING

A. System Model

A generic scenario of mixed vehicles on a highway with four lanes is depicted in Fig. 1, while an abstract model representation of Fig. 1 is shown in Fig. 2. A vehicle in the considered scenario can be a normal car V or a big vehicle B such as a bus or truck. We consider the length of the big vehicle to be L , while we consider its width w to be the same as the lane's width. We model the location of the vehicles by a hardcore repulsive Poisson Point Process (PPP).² If the road length is much longer than the lane width and vehicle length, and assuming that the vehicles moving on each lane are independent, we can combine four lanes into one PPP as shown in Fig. 2(b). We limit the Region of Interest (RoI) to D , which is the maximum communication range of a V2V link without any shadowing loss. The normal vehicle location distribution is a PPP with density β and the big vehicle location distribution is also a PPP, but with density λ_B .

B. Shadowing by Big Vehicles

In [15], we derived a closed-form solution for the shadow area caused by multiple big vehicles at random locations who follow a PPP distribution. Based on this, we can estimate whether a V2V

²For the analysis of vehicular networks in [4], [5], [6], [8], [19], [20], [21], a Poisson Point Process (PPP) is a commonly adopted model for vehicles due to its mathematical tractability [22]. However, vehicles have a physical size and cannot be considered as an ideal point. Furthermore, a vehicle has to keep a safe distance to other vehicles and objects, which means it exhibits the behavior of repulsive objects. To model vehicles on a straight road, we consider a safety space between two consecutive vehicles which were originally generated by a PPP. This tractable process is similar to a 1-dimensional Matérn hardcore point process [23], which is hence referred to as a hardcore repulsive PPP. This process describes a vehicle on a straight road with a minimum separation between two adjacent vehicles.

link is line-of-sight (LOS) or obstructed LOS (OLOS). If a V2V link is OLOS the two communicating vehicles are shadowed by a big vehicle. In this case the link will suffer a shadowing loss. In this paper, we consider that the big vehicle can be on any lane. A scenario of a pair of cars and a big vehicle can be on any of the four lanes we consider, leading to 64 cases of relative positions among them. To determine the average value of the shadowing region, we denote them as SD_{ijk} , and $i, j, k \in \{1, \dots, 4\}$, where i is lane of the tagged vehicle,³ j is the lane of the big vehicle, and k is the lane onto which the big vehicle will cast its radio shadow. Due to the symmetrical nature of the 4-lane road, we need to evaluate only 16 cases as follows⁴

$$SD_{111} = D - \frac{e^{-\frac{\lambda_B L}{2}}}{\lambda_B} (1 - e^{-\lambda_B D}) \quad (1)$$

$$SD_{112} = D - \frac{2e^{-\frac{\lambda_B L}{2}}}{\lambda_B} (1 - e^{-\frac{\lambda_B D}{2}}) \quad (2)$$

$$SD_{113} = D - \frac{4e^{-\frac{\lambda_B L}{2}}}{\lambda_B} (1 - e^{-\frac{\lambda_B D}{4}}) \quad (3)$$

$$SD_{114} = D - \frac{6e^{-\frac{\lambda_B L}{2}}}{\lambda_B} (1 - e^{-\frac{\lambda_B D}{6}}) \quad (4)$$

$$SD_{121} = 0 \quad (5)$$

$$SD_{122} = D + \frac{L}{2} + \frac{1}{\lambda_B} e^{-\frac{\lambda_B L}{2}} + \frac{2}{\lambda_B} e^{-\frac{\lambda_B D}{2}} - \frac{3}{\lambda_B} \quad (6)$$

$$SD_{123} = D - \frac{2}{3\lambda_B} (e^{-\frac{\lambda_B L}{2}} + e^{-2\lambda_B L}) + \frac{2}{\lambda_B} e^{-\frac{\lambda_B (D+2L)}{2}} \quad (7)$$

$$SD_{124} = D - \frac{1}{\lambda_B} (e^{-\frac{7\lambda_B L}{4}} + 2e^{-\frac{\lambda_B L}{4}}) + \frac{3}{\lambda_B} e^{-\lambda_B (\frac{D}{3} + \frac{3L}{4})} \quad (8)$$

$$SD_{131} = SD_{132} = 0 \quad (9)$$

$$SD_{133} = D + \frac{4}{\lambda_B} (e^{-\lambda_B (\frac{D}{4} + \frac{L}{8})} - e^{-\frac{3\lambda_B L}{8}}) + \frac{1}{\lambda_B} e^{-\frac{\lambda_B L}{2}} - \frac{L}{2} - \frac{1}{\lambda_B} \quad (10)$$

$$SD_{134} = D + \frac{3}{\lambda_B} (e^{-\lambda_B (\frac{D}{3} + L)} - e^{-\frac{5\lambda_B L}{3}}) + \frac{6}{5\lambda_B} (e^{-\frac{13\lambda_B L}{6}} - e^{-\frac{\lambda_B L}{2}}) \quad (11)$$

$$SD_{141} = SD_{142} = SD_{143} = 0 \quad (12)$$

$$SD_{144} = D + \frac{6}{\lambda_B} (e^{-\frac{\lambda_B D}{6}} - e^{-\frac{\lambda_B L}{6}}) + \frac{1}{\lambda_B} (e^{-\frac{\lambda_B L}{2}} - e^{-\frac{\lambda_B L}{2}}) \quad (13)$$

³The tagged vehicle is the transmitting vehicle at the origin, and all other vehicles on the road are considered as potential receivers. The performance metrics (e.g., shadow region) are used for evaluating the receiving quality of other vehicles from this tagged vehicle.

⁴A detailed explanation of the formulation of average shadowing regions is provided in Appendix.

All other cases can be derived from these equations. For example, $SD_{211} = SD_{122}$, $SD_{321} = SD_{123}$, etc.

From the average length of the shadowing regions, we can estimate the probability that a V2V link is under shadowing (OLOS). This probability is a function of the big vehicle density λ_B and can be calculated by

$$P_{\text{OLOS}} = \frac{\sum_{i=1}^4 \sum_{j=1}^4 \sum_{k=1}^4 SD_{ijk}}{64 \times D} \quad (14)$$

The probability of a V2V link being not under shadowing (LOS) is calculated by $P_{\text{LOS}} = 1 - P_{\text{OLOS}}$.

We can also calculate the probability that a V2V link is OLOS for a vehicle which is on the same lane as the big vehicle, or on the next lanes of the big vehicle. We denote these probabilities as $P_{\text{OLOS}}^{\text{Cat}0}$, $P_{\text{OLOS}}^{\text{Cat}1}$, $P_{\text{OLOS}}^{\text{Cat}2}$, $P_{\text{OLOS}}^{\text{Cat}3}$. It is expected that these probabilities are different and the closer the lane of the big vehicle, the higher the chance small vehicles (e.g., cars) are under the shadow of this big vehicle. Based on these probabilities, we can develop a strategy to select and help the car which is affected by the big vehicle shadow region.

C. Path-Loss Modeling

In order to evaluate the impact of big vehicle shadowing on car-to-car communication, we consider a channel model for the following two scenarios:

- Car-to-car communication with LOS channel condition.
- Car-to-car communication with LOS blocked by a big vehicle in between.

For the above scenarios, we consider the measurement-based path-loss models presented in [15], where a dual-slope path-loss model was built from measured data using linear regression. Specifically, the model for LOS is

$$PL_{\text{LOS}}(d_{t,r}) = \begin{cases} 57.2617 + 10 \times 1.5334 \log_{10} d_{t,r} + X_{\sigma_1} & d_{t,r} \leq 176.7 \text{ m} \\ 20.7653 + 10 \times 3.1202 \log_{10} d_{t,r} + X_{\sigma_2} & d_{t,r} > 176.7 \text{ m} \end{cases} \quad (15)$$

where X_{σ_1} and X_{σ_2} are zero mean Gaussian random variables with $\sigma_1 = 4.39$ dB and $\sigma_2 = 4.23$ dB. The coefficient of determination R^2 of the linear regression for the dual-slope path-loss model is 0.6601 and 0.9217, respectively. The high value of R^2 , especially of the steeper slope, shows the goodness of fit of the predicted model.

The model for OLOS is

$$PL_{\text{OLOS}}(d_{t,r}) = \begin{cases} 79.7089 + 10 \times 0.90925 \log_{10} d_{t,r} + X_{\sigma_1} & d_{t,r} \leq 176.7 \text{ m} \\ 28.3188 + 10 \times 3.1436 \log_{10} d_{t,r} + X_{\sigma_2} & d_{t,r} > 176.7 \text{ m} \end{cases} \quad (16)$$

where X_{σ_1} and X_{σ_2} are zero mean Gaussian random variable with $\sigma_1 = 1.74$ dB and $\sigma_2 = 1.24$ dB. In this case, the coefficient of determination R^2 is 0.616 and 0.9579, respectively. It can be observed that the difference between the expected path-loss of LOS and OLOS reaches 17 dB when the transmitter-receiver

distance is less than $d_c = 176.7$ m and reduces from 17 dB to 9 dB when this distance extends from d_c to 1000 m. The difference between the path-loss in these two models is caused by bus shadowing, and hence is referred to as shadowing loss for one big vehicle in this paper.

III. ANALYSIS OF CELLULAR V2X

Cellular-based vehicular communications (also known as C-V2X) has recently attracted significant attention due to its large coverage, high capacity, superior quality of services, and multicast/broadcast support. C-V2X communication exploits LTE uplink resources while utilizing Single Carrier Frequency Division Multiple Access (SC-FDMA) at the PHY and MAC layers [24]. According to the specifications, the available bandwidth is subdivided into equally-spaced (spacing of 15 kHz) orthogonal subcarriers. A Resource Block (RB) in LTE is formed by 12 consecutive subcarriers (i.e., 180 kHz) and one time slot (i.e., 0.5 ms). The number of data bits carried by each RB depends on the specific Modulation and Coding Schemes (MCS) selected.

To enable direct short-range communication between devices, C-V2X uses a direct communication interface, the PC5 interface (also known as side-link), which can be used for V2V and Vehicle-to-Infrastructure (V2I) communications. To utilize the available safety message resources, the current C-V2X communications operate in both network-controlled and autonomous modes. In the first mode (also known as Sidelink Mode 3), it is assumed that the vehicles are fully covered by one or more evolved NodeBs (eNBs), where eNBs dynamically assign the resources being used for V2V communications through control signalling. In the autonomous mode (also known as Sidelink Mode 4), vehicles are assumed to be in areas where no cellular coverage is available and hence, resources are allocated in a distributed manner. A sensing based semi-persistent transmission mechanism is introduced in Sidelink Mode 4 to enable distributed resource allocation. The distributed algorithm is implemented among the vehicles, which optimizes the use of the channel by increasing the resource reuse distance between vehicles that are using the same resources. In this work, we consider the autonomous resource allocation mechanisms (Sidelink Mode 4) with a sensing-based autonomous resource selection scheme.

A. Error Types in C-V2X Mode 4

In this paper, we utilize the analysis approach proposed in [25] for C-V2X Mode 4. It is important to note that the analysis in [25] encompasses a vehicular system with regular vehicles only. By focusing on big vehicles and the shadowing caused by them, this paper expands the C-V2X analysis presented in [25]. As pointed out in [25], there are four types of error that can affect Packet Delivery Ratio (PDR) performance analysis: errors due to half-duplex transmissions (HD) δ_{HD} , errors due to a received signal power below the sensing threshold δ_{SEN} , errors due to propagation effects δ_{PRO} , and errors due to packet collisions δ_{COL} . According to [25], these four types of error are mutually exclusive. When we calculate one type of error, we will exclude those quantified by the other errors. As big vehicle shadowing affects the above error types differently, the

followings subsections show how big vehicle shadowing impacts each error type.

1) *Half-Duplex Error*: The half-duplex error δ_{HD} is caused due to the half-duplex mechanism, in which a vehicle is unable to receive a packet while transmitting. δ_{HD} is independent of path-loss or shadowing, which can be calculated by:

$$\delta_{HD} = \Pr(e = HD) = \frac{\lambda}{1000}, \quad (17)$$

where λ is the packet transmission rate.

2) *Path-Loss and Fading Error*: This type of error happens when the received signal strength is below the decoding threshold. The received signal strength depends on the channel and is affected by shadowing losses caused by big vehicles. The path-loss and fading error in the presence of big vehicles is:

$$\begin{aligned} \delta_{SEN}^{OLOs}(d_{t,r}) &= \Pr(e = SEN | e \neq HD) \\ &= \frac{1}{2} \left(1 - \operatorname{erf} \left(\frac{P_t - PL^{OLOs}(d_{t,r}) - P_{SEN}}{\sigma\sqrt{2}} \right) \right), \end{aligned} \quad (18)$$

where $d_{t,r}$ is the distance between transmitter and receiver, P_t is the transmit power, $PL^{OLOs}(d_{t,r})$ is the path-loss from the transmitter to the receiver, P_{SEN} is the sensing and decoding threshold, σ is the standard deviation of the large-scale fading distribution, erf is the error function.

Note that the complementary part of δ_{SEN} is the Packet Sensing Ratio (PSR), $PSR = 1 - \delta_{SEN}$.

3) *Propagation Error*: This error is due to the propagation effects that influence the PHY layer performance at the receiver. For a given range of Signal-to-Noise-Ratio (SNR), an estimation of propagation error can be obtained from a lookup table when the SNR is within a certain range, where the SNR depends on the channel quality between transmitter and receiver. With big vehicle shadowing, the propagation error can be calculated as:

$$\begin{aligned} \delta_{PRO}^{OLOs}(d_{t,r}) &= \Pr(e = PRO | e \neq HD, e \neq SEN) \\ &= \sum_{s=-\infty}^{+\infty} BL(s) \cdot f_{SNR^{OLOs}|P_r > P_{SEN}, d_{t,r}}(s), \end{aligned} \quad (19)$$

where

$$f_{SNR^{OLOs}|P_r > P_{SEN}, d_{t,r}}(s) = \begin{cases} \frac{f_{SNR^{OLOs}, d_{t,r}}(s)}{1 - \delta_{SEN}} & \text{if } P_r > P_{SEN} \\ 0 & \text{if } P_r \leq P_{SEN} \end{cases},$$

where $BL(s)$ is the block error rate for an SNR equal to s , $f_{SNR^{OLOs}, d_{t,r}}(s)$ is the probability density function (PDF) of the SNR experienced at a distance $d_{t,r}$ for those SNR values for which P_r is higher than P_{SEN} . We know that the SNR at the receiver is $SNR^{OLOs}(d_{t,r}) = P_t - PL^{OLOs}(d_{t,r}) - P_{fading} - N_0$, hence the PDF of the SNR will follow the log-normal distribution of fading P_{fading} with a new mean value $P_t - PL^{OLOs}(d_{t,r}) - N_0$,

$$\begin{aligned} &f_{SNR^{OLOs}, d_{t,r}}(s) \\ &= \frac{1}{\sigma\sqrt{2\pi}} \exp \left(- \left(\frac{P_t - PL^{OLOs}(d_{t,r}) - N_0 - s}{\sigma\sqrt{2}} \right)^2 \right). \end{aligned}$$

4) *Packet Collision Error*: Error due to packet collisions is observed whenever two vehicles with insufficient channel sensing information choose to transmit their packets on the same transport block. In the event of a packet collision, a receiver cannot decode the collided data packet if the Signal-to-Interference and Noise-Ratio (SINR) of desired packet is lower than the threshold. Thus, the packet collision error δ_{COL} relies on a semi-persistent sensing mechanism and received SINR, while both of these factors are influenced by the channel. Thus, the packet collision error δ_{COL} is determined by the semi-persistent sensing mechanism and the received SINR, while the channel influences both of these aspects. With big vehicle shadowing, δ_{COL} is given by,

$$\begin{aligned} \delta_{COL}^{OLOS}(d_{t,r}) &= \Pr(e = COL | e \neq HD, e \neq SEN, e \neq PRO) \\ &= 1 - \prod_i \left(1 - \delta_{COL}^{OLOS,i}(d_{t,r}, d_{t,i}, d_{i,r})\right), \end{aligned} \quad (20)$$

where

$$\delta_{COL}^{OLOS,i}(d_{t,r}, d_{t,i}, d_{i,r}) = p_{SIM}^{OLOS}(d_{t,i}) \cdot p_{INT}^{OLOS}(d_{t,r}, d_{i,r}), \quad (21)$$

where $p_{SIM}^{OLOS}(d_{t,i})$ is the probability that the tagged vehicle (transmit vehicle) v_t and interfering vehicle v_i simultaneously transmit using the same resource. $p_{INT}^{OLOS}(d_{t,r}, d_{i,r})$ is the probability that the interference generated by v_i at receiver v_r is higher than a threshold, which means v_r cannot decode correctly. $d_{t,i}$ and $d_{i,r}$ are the distance between the interfering vehicle and the transmitter and receiver vehicles, respectively. The SINR at receiving vehicle is

$$SINR(d_{t,r}, d_{i,r}) = g_D \cdot P_r(d_{t,r}) - P_i(d_{i,r}) - N_0, \quad (22)$$

where g_D is the antenna directivity gain,⁵ $P_r(d_{t,r})$ is the received power from transmitting vehicle, $P_i(d_{i,r})$ is the received power from interfering vehicle, and N_0 is the noise power.

The second probability is calculated by

$$p_{INT}^{OLOS}(d_{t,r}, d_{i,r}) = \frac{p_{SINR}^{OLOS}(d_{t,r}, d_{i,r}) - \delta_{PRO}^{OLOS}(d_{t,r})}{1 - \delta_{PRO}^{OLOS}(d_{t,r})}, \quad (23)$$

$$\begin{aligned} p_{SINR}^{OLOS}(d_{t,r}, d_{i,r}) \\ = \sum_{s=-\infty}^{+\infty} BL(s) \cdot f_{SINR^{OLOS}|P_r > P_{SEN}, d_{t,r}, d_{i,r}}(s), \end{aligned} \quad (24)$$

the $f_{SINR^{OLOS}|P_r > P_{SEN}, d_{t,r}, d_{i,r}}(s)$ is the PDF of SINR and calculated from the cross correlation of the PDF of P_r and P_i [25].

The first probability is calculated by a complex two step procedure derived from sensing-based semi-persistent scheduling (SPS).

$$p_{SIM}^{OLOS}(d_{t,i}) = \alpha \cdot p_{SIM}^{[2]}(d_{t,i}) + (1 - \alpha) \cdot p_{SIM}^{[3]}(d_{t,i}), \quad (25)$$

where the factor α is empirically chosen from the channel busy ratio (CBR), and $p_{SIM}^{[2]}$ and $p_{SIM}^{[3]}$ denote the probability of

⁵For omni-direction reception $g_D = 1$, and thus, the high directivity antenna can help to improve the SINR.

simultaneous transmission in step 2 and 3 of the SPS protocol.

$$p_{SIM}^{[2]}(d_{t,i}) = p_s(d_{t,i}) \cdot \frac{C_C(d_{t,i})}{N_C^2} \quad (26)$$

$$p_s(d_{t,i}) = 1 - \left(1 - \frac{1}{\tau}\right) \cdot PSR(d_{t,i}) \quad (27)$$

$$PSR(d_{t,r}) = \frac{1}{2} \left(1 + \operatorname{erf}\left(\frac{P_t - PL(d_{t,r}) - P_{SEN}}{\sigma\sqrt{2}}\right)\right) \quad (28)$$

$$C_C(d_{t,i}) = C_A(d_{t,i}) \cdot \left(\frac{N_C}{N_A}\right)^2 \quad (29)$$

$$C_A(d_{t,i}) = N - 2 \cdot N_E + C_E(d_{t,i}) \quad (30)$$

$$N = 1000 \cdot \frac{S}{\lambda} \quad (31)$$

$$N_E = \frac{S_{PSR}}{2} + \sum_{k=1}^{S_{PSR}/2} \max\left(1 - \frac{k}{1 - \frac{S_{PSR}}{2}}, 0\right) \quad (32)$$

$$\begin{aligned} S_{PSR} &= \sum_{i=-\infty}^{\infty} PSR(d_{t,i}) = \sum_{i=-\infty}^{\infty} PSR\left(\frac{i}{\beta}\right) \\ &= \beta \cdot \sum_{i=-\infty}^{\infty} PSR(i) \end{aligned} \quad (33)$$

$$C_E(d_{t,i}) = \frac{R_{PSR}(d_{t,i})}{R_0} \left(\frac{\beta N_E R_0}{S_{PSR}} - \frac{N_E^2}{N}\right) + \frac{N_E^2}{N} \quad (34)$$

$$R_{PSR}(d_{t,i}) = \sum_{j=-\infty}^{\infty} PSR\left(\frac{j}{\beta} + d_{t,i}\right) PSR\left(\frac{j}{\beta}\right) \quad (35)$$

$$p_{SIM}^{[3]}(d_{t,i}) = p_s(d_{t,i}) \cdot \frac{C_C(d_{t,i})}{N_C^2} \quad (36)$$

$$\frac{S_{PSR}^{(n)}}{2} + \sum_{k=1}^{S_{PSR}^{(n)}/2} \max\left(1 - \frac{k}{1 - \frac{S_{PSR}^{(n)}}{2}}, 0\right) \leq 0.8 \cdot N \quad (37)$$

$$S_{PSR}^{(n)} = \sum_{i=-\infty}^{\infty} PSR\left(\frac{i}{2\beta}\right) = 2\beta \cdot \sum_{i=-\infty}^{\infty} PSR(i) \quad (38)$$

$$\begin{aligned} PSR_n(d_{t,r}) \\ = \frac{1}{2} \left(1 + \operatorname{erf}\left(\frac{P_t - PL(d_{t,r}) - (P_{SEN} + n \cdot \Delta)}{\sigma\sqrt{2}}\right)\right), \end{aligned} \quad (39)$$

where p_s is the probability that two nodes cannot sense each others (hidden terminal scenario), τ is the average number of consecutive packet transmissions, PSR is the packet sensing ratio, which is the ratio of received packet to total number of transmitted packet. C_C is the number of common candidate resources, C_A is the number of common assignable resources, C_E is the number of common excluded resources, N is a total number of resources in the selection window, N_E is the number of resources excluded in Step 2 of sensing-based SPS. N_A is the number of assignable resources, N_C is the number of

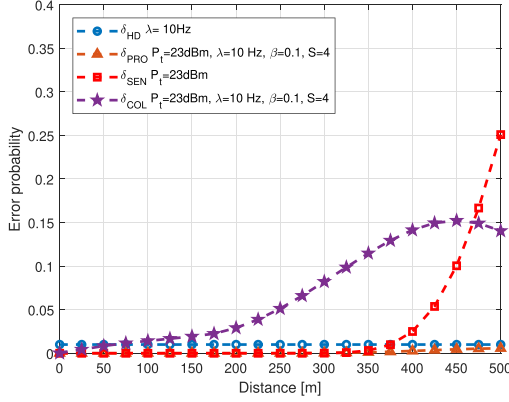


Fig. 3. Probability of occurrence of different types of errors in C-V2X.

candidate resources that can be used after Step 2 and 3, where $N_C = 20\%N$, S are the number of sub-channels per sub-frame, Δ is the step size in an iteration where the number of selected resources reach 80% of the available resource pool. In the packet error due to the collision scenario, shadowing plays a big role in calculating the packet sensing ratio PSR .

These four types of error are derived from parameters in [25] and illustrated in Fig. 3. At a distance less than 450 m, the packet collision error is dominant. If the distance between transmitter and receiver is larger than 450 m, the path-loss and fading error form a major part. These two types of error are more severe when there is big vehicle shadowing because the shadowing loss reduces both communication and sensing ranges. In the presence of big-vehicle shadowing, these two major errors will be further aggravated. Therefore, we propose techniques to alleviate them in this paper.

B. Packer Delivery Ratio Performance

The Packet Delivery Ratio (PDR) is directly derived⁶ from the four types of error described in the earlier subsection.

$$PDR(d_{t,r}) = (1 - \delta_{HD}) (1 - \delta_{SEN}(d_{t,r})) (1 - \delta_{PRO}(d_{t,r})) \quad (40)$$

$$(1 - \delta_{COL}(d_{t,r}))$$

$$PDR(d_{t,r}) = 1 - \hat{\delta}_{HD} - \hat{\delta}_{SEN} - \hat{\delta}_{PRO} - \hat{\delta}_{COL} \quad (41)$$

$$\hat{\delta}_{HD} = \delta_{HD} \quad (42)$$

$$\hat{\delta}_{SEN}(d_{t,r}) = (1 - \delta_{HD})\delta_{SEN}(d_{t,r}) \quad (43)$$

$$\hat{\delta}_{PRO}(d_{t,r}) = (1 - \delta_{HD})(1 - \delta_{SEN}(d_{t,r}))\delta_{PRO}(d_{t,r}) \quad (44)$$

$$\hat{\delta}_{COL}(d_{t,r}) = (1 - \delta_{HD})(1 - \delta_{SEN}(d_{t,r})) \quad (45)$$

$$(1 - \delta_{PRO}(d_{t,r}))\delta_{COL}(d_{t,r})$$

$$0 \leq \delta_{HD}, \delta_{SEN}, \delta_{PRO}, \delta_{COL} \leq 1 \quad (46)$$

⁶Note that independence between errors is assumed in the overall PDR derivation. While dependency may be observed between different error components (for example, path loss and propagation errors are both impacted by shadowing), the impact due to the dependency is negligible.

In the absence of big vehicles, all types of error (i.e., δ_{HD} , δ_{SEN} , δ_{PRO} , δ_{COL}) are calculated based on the LOS channel model. On the other hand, the shadowing model is used in the presence of a big vehicle to determine those errors. The PDR for this scenario is

$$PDR^{OLOS}(d_{t,r}) = 1 - \hat{\delta}_{HD} - \hat{\delta}_{SEN}^{OLOS} - \hat{\delta}_{PRO}^{OLOS} - \hat{\delta}_{COL}^{OLOS}. \quad (47)$$

For traffic of mixed vehicle type on the road, the overall PDR performance is calculated by

$$PDR(d_{t,r}) = P_{OLOS} \cdot PDR^{OLOS} + (1 - P_{OLOS}) \cdot PDR^{LOS}, \quad (48)$$

where P_{OLOS} is as per (14).

In the relaying scenario, we assume that two hops of the relaying link are LOS because of the high antenna position on the big vehicle. The performance of each hop follows the performance analysis of the LOS link. The relaying link introduces one retransmission and is equivalent to introducing one more node in the network. Thus, the effective vehicle density becomes

$$\beta_{\text{eff}} = (1 + P_{OLOS})\beta. \quad (49)$$

IV. PROPOSED PHY STRATEGY: DUAL-BEAM RECEPTION

It is well known that the performance of a sensing-based multiple access wireless system is heavily affected by packet collisions caused by hidden nodes [25], [26]. In [25], authors report that at the communication distance below 400 m, the error caused by this packet collision is dominant. For example, packet collision causes a packet error probability of 0.38 at 380 m, while half-duplex and propagation issues cause errors with probability of 0.01 and 0.006, respectively. The packet collision evidently degrades the performance of the vehicular network in broadcast mode, where no Request-To-Send/Clear-To-Send mechanism is applied. In a vehicular network, packets collided at the receiving vehicle usually belong to a vehicle at the front and a vehicle at the back. If the receiving vehicle can distinguish the packets from the front and the back directions, it can generally overcome the hidden node problem.

In this paper, we propose a beamforming-based signal reception mechanism using an antenna array with two omni-direction elements only. This antenna array can be used for all kinds of vehicles, either big vehicles such as trucks, buses, vans or normal vehicles such as a car. The proposed beamforming approach is a suitable solution for a vehicle needing to receive packets that were simultaneously transmitted from a front vehicle and a rear vehicle.⁷ Let us consider an array of two isotropic antennas separated by a distance d along x -axis. The total field of the array is the product of the field of a single antenna element with the array factor [27]. If we apply a weighting factor $w_1 = [1 \ j]$ and $w_2 = [1 \ -j]$ for each element, the normalized array factors at elevation angle $\theta = 90^\circ$ are

$$AF_1 = \frac{1}{2} \left[e^{j(kd \cos \phi + \beta)/2} + j e^{-j(kd \cos \phi + \beta)/2} \right] \quad (50)$$

⁷Though an antenna array with a large number of elements can steer a narrow beam into specific directions, such an array is more suitable for use at the base station due to its size and latency in beam switching.

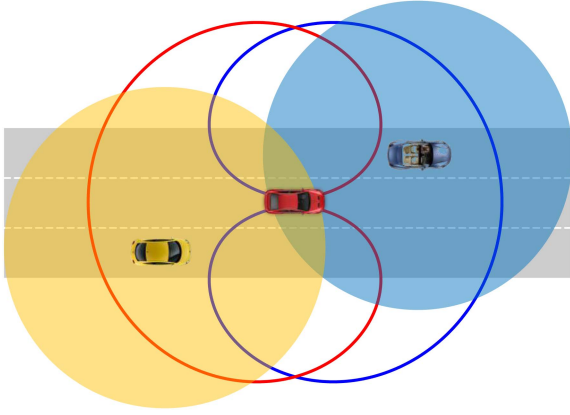


Fig. 4. Antenna beams of front and back antennas of the red vehicle.

$$AF_2 = \frac{1}{2} \left[e^{j(kd \cos \phi + \beta)/2} - j e^{-j(kd \cos \phi + \beta)/2} \right] \quad (51)$$

respectively, where $kd = 2\pi d/\lambda$, λ is the wavelength, ϕ is the azimuthal angle, and β is the phase between two elements. If we set the element separation $d = \lambda/4$ and the phase $\beta = 0$, the normalized amplitude of the array factors are

$$|AF_1|_n = 1 + \sin\left(\frac{\pi}{2} \cos \phi\right) \quad (52)$$

$$|AF_2|_n = 1 - \sin\left(\frac{\pi}{2} \cos \phi\right). \quad (53)$$

By placing the array antenna axis along the length of the vehicle, we can observe that the radiation pattern with weighting factor w_1 will be facing the front of the vehicle, while the radiation pattern with weighting factor w_2 will be facing the back of the vehicle, as illustrated in Fig. 4. Note that in spite of the leakage (i.e., back-lobe) in the opposite direction, we see a substantial gain in directivity. By defining the directivity gain g_D as the ratio of array factors, the g_D in dB is given by,

$$g_D = 20 \log \frac{|AF_1|_n}{|AF_2|_n}, \quad (54)$$

and illustrated in Fig. 5 a.

Fig. 5 b illustrates a g_D map of the front and back of a bus (12 m length by 3.5 m width) travelling on a six-lane highway (21 m total width). With the designed antenna array, signals can be received from two opposite directions in a highly directive manner. For calculating the received signal in a single direction, we can apply (54). The gain is infinity when the azimuth ϕ is 0° or 180° . At this angle, the radiation in the opposite direction is null. The directivity gain is as small as 0 dB when the ϕ is around -90° and 90° , which are the rear areas of the vehicle. We observe that the high directivity of the proposed antenna array can increase SINR at the receiving vehicle (see (22)) to prevent packet collisions that result from hidden nodes.

V. PROPOSED MAC STRATEGIES: RELAYING BY BIG VEHICLES

A number of previous works, such as [7], [8], [10], [12], [28] have demonstrated how vehicle shadowing affects the received signal. In the report of a field trial [29], it was shown that a

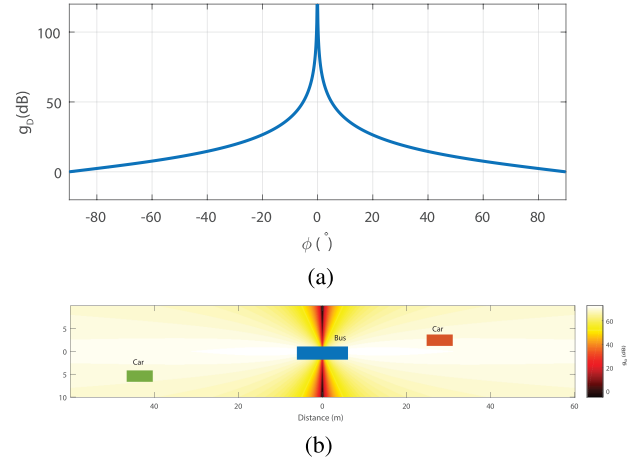


Fig. 5. Directivity gain g_D . (a) Directivity gain over azimuth. (b) Illustration of g_D of the big blue vehicle with true-scale vehicle sizes.

medium sized truck followed by a sedan car can reduce the communication range of the car significantly (i.e., communication range is reduced from 900 m to 200 m). On the other hand, the shadowing by big vehicles reduces the sensing range and makes the hidden node problem more serious. Thus, there is a need for relaying techniques, that can extend the communication range without consuming much system resources or introducing much interference. To utilize resources effectively, a big vehicle⁸ will

- relay the packets belonging to the vehicles under its shadow only,
- not relay for vehicles under its shadow, whose packets are relayed by another big vehicle.

In this paper, we propose three smart relaying techniques which are applied at big vehicles to mitigate the negative impact of big vehicle shadowing and to meet the above goals. Each of the proposed relaying schemes is discussed in detail in the following.

A. Front-Back Relaying (FB-Relaying)

This technique relies on dual beamformed radiation of an antenna array (as described in IV), which allows a big vehicle to receive packets at the front and retransmit from the back and vice versa, e.g. a big vehicle can receive the data at its front antenna by using weighting factor w_1 and retransmit from its back by using weighting factor w_2 and vice versa. A simple example of this relaying technique is given below. A big vehicle, for example B_1 in Fig. 2.b will relay the data packet of V_1 to the front of it (i.e., right hand side of B_1) and relay data packet of V_2 to the back of it (i.e., left hand side of B_1). B_1 will not retransmit omni-directionally, for example, for V_2 because V_2 and V_3 are not a pair under B_1 's shadow. In this situation, big vehicle B_2 will monitor the relayed data packet. If B_2 receives a relayed packet from V_1 through B_1 , it will not relay for V_1 to the right

⁸Since big vehicles can achieve larger communication ranges than normal vehicles due to the high antenna position, we consider that the big vehicle performs the relaying tasks.

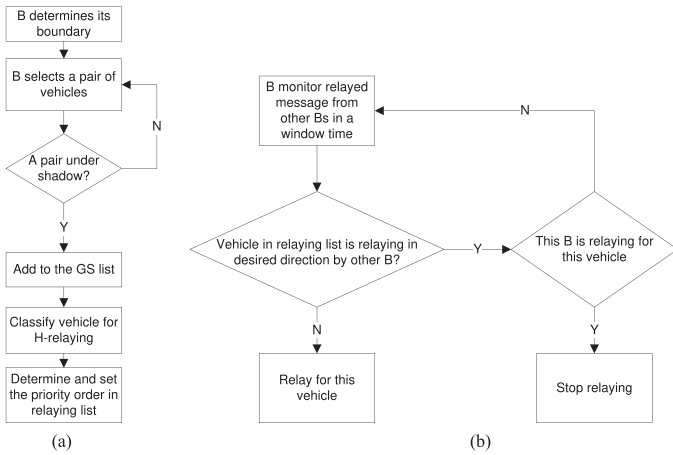


Fig. 6. Algorithms: (a) Selecting shadowed vehicle to relaying list, and (b) Monitoring other B s relaying to make relaying decision.

hand side. This mechanism is to avoid spending system resource for redundant packets.

A flow chart of the proposed relaying mechanism is shown in Fig. 6. In a first step, a big vehicle creates a list containing IDs of normal vehicles that are under its geometrical shadow. The shadow boundary of a big vehicle can be modeled as a convex polygon based on its Global Navigation Satellite System (GNSS) data and its size. Upon receiving locations of normal vehicles through exchanged messages (e.g., BSM), the big vehicle forms a line between two points corresponding to the location of two normal vehicles. When the big vehicle receives normal vehicles' locations through message exchanges (e.g., BSM), a line is formed to connect two points representing locations of two normal vehicles. If the line cuts the polygon, those normal vehicles are considered under the shadow of the big vehicle, and they are added to the geometrically shadowed (GS) vehicle list. After building the GS list, the big vehicle needs to monitor relayed packets by other big vehicles to make relaying decision in the second phase. The big vehicle will not relay a packet from a normal vehicle in GS list, if another big vehicle has already relayed that packet in the desired direction. This mechanism can be illustrated by example in Fig. 2: if B_2 receives a relayed packet from V_1 through B_1 , B_2 will not relay for V_1 and if B_2 is relaying for V_1 , B_2 will stop the relaying process.

B. Lane-Selective Hierarchical Relaying (H-Relaying)

In the event of many normal vehicles being located under a big vehicle's shadow or limited system resources, the big vehicle will have to prioritize and relay packets of some critical vehicles first. It can cut down the number of retransmission⁹ and reduce the relaying load for big vehicle. We propose a mechanism called Lane-Selective Hierarchical Relaying (H-relaying) to allow big vehicles to selectively relay for cars that are impacted by shadowing more than others.

⁹For a given relaying scenario, the number of retransmissions is defined by the number of transmissions made from the big vehicles.

From the shadowing analysis, we observe that shadowing is strongly influenced by the proximity of a big vehicle's lane and a normal vehicle's lane. For example, when a big vehicle and a normal vehicle are on the same lane, the normal vehicle suffers a larger shadow region and thus, worse channel quality is observed for compared to other vehicles. By taking this fact into account, we classify normal vehicles as follow

- Cat0 vehicles: vehicles are on the same lane with the big vehicle
- Cat1 vehicles: vehicles are on the next lane to the big vehicle
- Cat2 vehicles: vehicles are two lanes away from the big vehicle
- and so on.

Based on the locations of the vehicles (obtained through GNSS) and the lane width, a big vehicle can determine the lane of a normal vehicle. The big vehicle can draw a baseline which goes through the center from its front to back, then calculate the distance of a normal vehicle to this baseline. Comparing this distance to the lane width, the big vehicle can establish the lane of a specific normal vehicle. When a big vehicle implements FB-relaying, it can choose to relay for a group of vehicles in different categories as follows

- H-relaying Cat0: relay for vehicles that are on the same lane as the big vehicle
- H-relaying Cat1: relay for vehicles that are in H-relaying Cat0 and vehicles that are on the next lane to the big vehicle
- H-relaying Cat2: relay for vehicles that are in H-relaying Cat1 and vehicles are two lanes away from the big vehicle
- and so on,

where its probability of V2V link under the big vehicle shadowing is derived in part II-B.

C. Network Coding Based on Geometrically Shadowing Relaying (NCG-Relaying)

Since the antenna array can receive/transmit in both directional and omni-direction manners, we propose a network-coded relaying scheme based on geometrical shadowing (NCG-relaying) to reduce the number of retransmission. In the earlier relaying schemes (i.e., FB-relaying), a big vehicle needs two transport blocks to retransmit packets from two normal vehicles (one located at the front of the big vehicle and the other at the back). In NCG-relaying, only one packet needs to be retransmitted by the big vehicle, which is an X-OR combination of original packets from the two normal vehicles. When a normal vehicle receives the network-coded packet and knows one of the two original packets, it can decode the received packet to get the remaining packet. For example, in Fig. 2.b, when V_3 receives a network-coded packet from V_1 and V_2 through B_1 , V_3 will be able to decode the network-coded packet to get V_1 's packet, because it is highly likely that V_3 can receive packets from V_2 due to the LOS link. In comparison with FB-relaying, the NCG-relaying uses 50% less transport blocks (TBs) in the re-transmission phase, which reduces network traffic and packet collisions.

TABLE I
SIMULATION PARAMETERS

Parameter	Value
Number of lane	4
Lane width w	3 m
Region of interest	500 m
Big vehicle's length L	12 m
Big vehicle's density λ_B	0-0.04 B Veh/m
Normal vehicle density β	0.1, 0.2, 0.3 Veh/m
Transmit power P_T	23 dBm
Path-loss at reference point P_0	[42.4317 3.5505] dB
Path-loss attenuation n	[2.27 4]
Log-normal fading std. dev. σ	3 dB
Carrier frequency	5.91 GHz
Bandwidth	10 MHz
Receiver sensitivity P_{SEN}	-90.5 dBm
Noise power	-95 dBm
Packet rate λ	10 Hz
Packet size B	190 Bytes
Sub-channel per sub-frame S	4
RBs per sub-channel	12
MCS	MCS9 (QPSK 0.7)

TABLE II
A HIGH-LEVEL COMPARISON OF THE PROPOSED RELAYING SCHEMES

Relay scheme	FB-Relaying	H-Relaying	NCG-Relaying
PDR performance w.r.t. FB-Relaying	–	Similar	Slightly worse
Message relay load	High	Medium	Low
Requirement of accurate lane information	✗	✓	✗
Requirement of self-interference cancellation	✗	✗	✓

VI. PERFORMANCE EVALUATION AND DISCUSSION

To evaluate the impact of big vehicle shadowing on C-V2X V2V communications and the efficiency of each relaying method, we carry out a numerical analysis using Matlab. Our system is a highway model with four-lane street (2 lanes per driving direction) as mentioned in [25]. Normal car and big vehicle locations follow a Poisson Point Process (PPP) [15], [25]. The parameters used in the simulation are summarized in Table. II. For fair comparison, we have chosen the same parameters as in [25], where big vehicle shadowing was not taken into account.

A. Impact of Big Vehicle Shadowing

In order to evaluate the probability of big vehicle shadowing, we carry out simulations in Matlab and compare simulation results with the analysis results in part II-B. Vehicle locations on the 4-lane road follow a Poisson Point Process, where the big vehicle density on each lane varies from 0.001 to 0.01. The big vehicle will cast the shadowing region on each lane

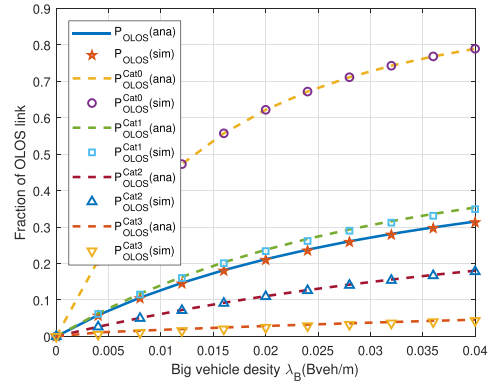


Fig. 7. Probability that a V2V link is being shadowed (OLOS).

and the average value of non-overlapped shadowing regions is calculated. The simulation results are derived from 50,000 trials and compared with the analytical results. Both results are shown in Fig. 7.

Fig. 7 shows the probability of a V2V link being subjected to big vehicle shadowing (i.e., OLOS link). Shadowing probabilities are calculated for each category of vehicles as well as for the overall scenario. We observe that a V2V connection (between two normal vehicles) is more likely under the shadow (i.e., P_{OLOS} increases) when the density of big vehicles, e.g. λ_B , increases. On average, the probability of an OLOS link increases from 0 to 0.31, when λ_B increases from 0 to 0.04. However, there is a variation in the probability of an OLOS link depending on where the normal vehicle is located relative to the big vehicle. If a normal vehicle is in the same lane as the big vehicle (i.e., when the normal vehicle falls into the Cat0 vehicles), P_{OLOS} increases from 0 to 0.79 when λ_B increases from 0 to 0.04. The shadowing probability is significantly lower when the lane of a normal vehicle is far away from the lane of the big vehicle. For example, the maximum shadowing probability values for Cat1, Cat2, and Cat3 vehicles are 0.35, 0.18 and 0.045, respectively. In light of these different probabilities, it is evident that big vehicles have a different impact on normal vehicles. Therefore, the big vehicle can set different priorities in the selective relaying strategy.

B. Benefit of Dual-Beam Reception Strategy

In Fig. 8, we present the effectiveness of the proposed dual receive beamforming strategy (as described in Section IV) in the V2V communications. For simplicity, we first analyze the PDR performance without dual receive beamforming. For different vehicle densities, we observe a sharp decay in the PDR when the distance increases. Although the PDR is affected by four types of error, the main contribution to the degradation of PDR is from packet collisions and low received signal strength due to path-loss and fading error. From [25], we know that the packet collisions due to the hidden-node problem dominate the packet error when the distance is over 300 m. Furthermore, increasing vehicle density also degrades PDR, as higher vehicle density causes hidden-node packet collision errors to increase. When the vehicle density increases from 0.1 to 0.3, we observe a decrease

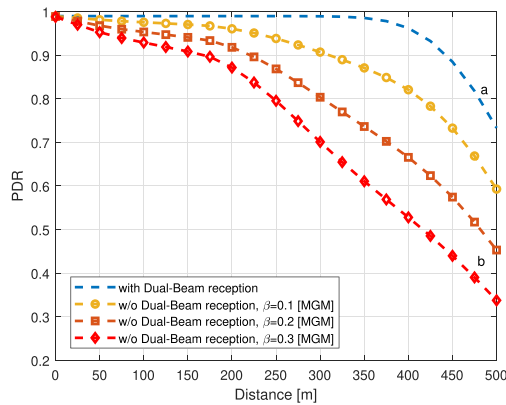


Fig. 8. PDR of system without big vehicle shadowing in comparison with the results derived from [25] (i.e., MGM in the figure).

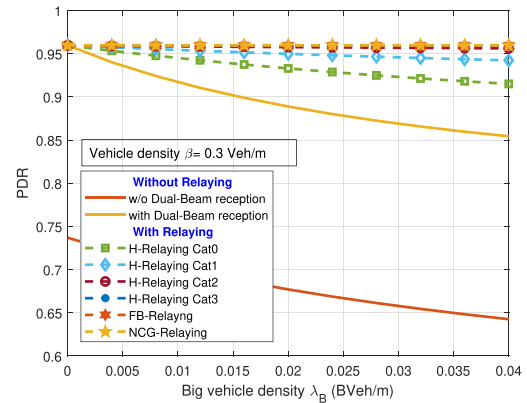


Fig. 10. PDR versus big vehicle density.

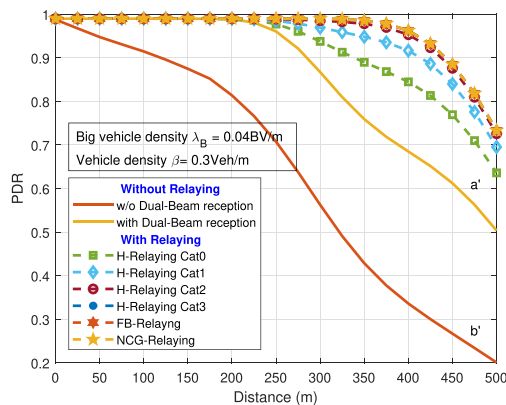


Fig. 9. PDR versus the TX-RX distance with big vehicle shadowing.

in PDR from 0.6 to 0.34 at distance of 500 m. On the other hand, by applying the dual receive beamforming approach, the PDR performance can be significantly improved. The receive beamforming PDR keeps as high as 0.99 when the distance is below 350 m. While PDR starts to drop after 350 m, the proposed dual receive beamforming strategy significantly outperforms a setup without receive beamforming scenarios. This benefit stems from the fact that dual receive beamforming can effectively handle the hidden nodes. It allows to decode two packets which are simultaneously transmitted from two sides of a receiver even if the same transport block is assigned to the transmitted packets.

C. Performance of the Proposed Relaying Schemes

Fig. 9 shows the PDR performance of the proposed relaying techniques in the big vehicle shadowing environment. In this scenario, we fix the normal vehicle density $\beta = 0.3$ veh/m and the big vehicle density $\lambda_B = 0.04$ B Veh/m.

In comparison to the results shown in Fig. 8, the OLOS worsens the PDR degradation. Let us compare the PDR curves without receive beamforming and relaying, PDR-b in Fig. 8 and PDR-b' in Fig. 9. The PDR of the system with big vehicle shadowing is only 0.2 at a distance of 500 m while it is more than 0.3 when there is no big vehicle shadowing. It is clearer that when all vehicles use receive beamforming, the PDR-a in

Fig. 8 can reach more than 0.7 at 500 m, while the PDR-a' in Fig. 9 is only 0.5 at the same distance. The path-loss on a V2V communication link is further impacted by the big vehicle shadowing, which leads to the degradation of PDR. Additionally, the reduced sensing range due to big vehicle shadowing causes more packet collisions. Therefore, even for distances as short as 50 m, the PDR starts to drop. In the presence of receive beamforming, the PDR is up to 0.99 and remains constant for a distance of up to 200 m. We observe a drastic drop in PDR after 200 m. It is possible to keep a high PDR for a longer distance by employing the proposed relaying schemes. Out of the relaying schemes proposed, FB-relaying and NCG-relaying exhibit similar PDR performance. At 350 m, the PDR of both relaying schemes is around 0.98, while at 500 m, the PDR is around 0.73. Note that NCG-relaying consumes less system resources than the FB-relaying scheme since FB-relaying requires more retransmissions than NCG-relaying. However, NCG-relaying is computationally more expensive than FB-relaying as NCG-relaying needs X-OR encoding at the transmitter and X-OR decoding at the receiver. Finally, one can also select H-relaying to limit the number of retransmissions.

The performance of H-relaying Cat3 is similar to that of FB-relaying, as the big vehicles relay packets for all normal vehicles in both scenarios. While the performance of H-relaying Cat2 is very close to FB-relaying, the former can reduce the relaying task for normal vehicles as the big vehicles do not need to relay packets that are generated from normal vehicles in the furthest lane. The performance of H-relaying Cat1 and Cat0 are next to the performance of H-relaying Cat2, while the relaying task is significantly reduced in H-relaying Cat1 and Cat0 scenarios. For example, in the H-relaying Cat0 scenario, the big vehicles only need to relay for normal vehicles that are on the same lane.

In Fig. 10, we show the PDR performance while varying the big vehicle density λ_B and setting a fixed vehicle density ($\beta = 0.3$ Veh/m). The overall PDR result is achieved by averaging the PDR results for distances from 0 to 500 m. The receive beamforming can only improve the PDR from 0.65 to 0.85 at $\lambda_B = 0.04$. The relaying techniques help to increase PDR performance further. The light-weight H-relaying Cat0 increases

PDR to more than 0.91, while others can increase the PDR to more than 0.96.

A high-level comparison of the proposed relaying schemes is summarized in Table II. FB-relaying and NCG-relaying exhibit almost the same PDR performance, while perform slightly better than H-relaying. Since NCG-relaying needs the receiving vehicle to do self-interference cancellation, FB-relaying is recommended over NCG-relaying. However, FB-relaying puts high processing load on On-Board-Unit (OBU), which may not be feasible in some scenarios. In such cases, H-relaying can be adopted to reduce the relaying load, provided that lane information is available.

VII. CONCLUSION

In this paper, we have analyzed the impact of big vehicle shadowing impacts V2V communications in the Mode-4 C-V2X networks. Using the lane-specific shadowing probability functions, a big vehicle shadowing model is presented, which is beneficial in developing lane-hierarchical strategies to tackle the communication performance degradation caused by big vehicle shadowing. An analysis is performed to examine the impact of vehicle shadowing on V2X communication links by considering the different types of errors that can arise within C-V2X networks. We have proposed a beamforming-based signal reception technique which is applied to all types of vehicles in order to reduce packet collisions due to hidden nodes. At a transmission distance of 500 m, dual receive beamforming can improve the PDR performance by 117.6%. We have also proposed three relaying algorithms, named FB-relaying, H-Relaying and NCG-Relaying, to enhance the V2V message dissemination effectiveness. A geometrical shadowing region selection protocol combined with these relaying techniques compensates for the communication degradation caused by vehicle shadowing. We have shown that the relaying techniques can improve the PDR performance from 0.2, where no relaying is applied, to 0.63 or 0.73 depending on which relaying technique is used. In the future, it will be interesting to consider more sophisticated distributions of big vehicles with different heights and lengths.

APPENDIX

In this part, a formulation of the average shadowing region of big vehicles is shown. We derive this for two cases SD_{112} and SD_{122} in detail. The same method can be applied to the remaining cases as well.

A. SD_{112} Formulation

We assume the tagged vehicle is at origin 0 on lane one. The length and width of big vehicle B are L and w respectively, where the center point of B is modeled by a 1-dimensional homogeneous PPP with density λ_B . The big vehicle B , located at position x_B on lane one, will cast the geometrical shadow region on lane two from point Q to point D is the end of region of interest as shown in Fig. 11. We can see that the two right angle triangles OMN and NPQ are equal. The position of point M is at

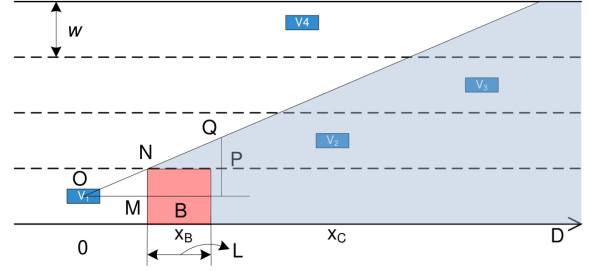


Fig. 11. Geometrical shadowing SD_{112} .

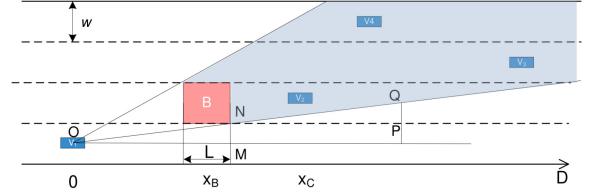


Fig. 12. Geometrical shadowing SD_{122} .

$(x_B - L/2)$, while the position of point Q is at $2(x_B - L/2)$. The geometrical shadow region on lane two is from $(2x_B - L)$ to D .

Considering a normal vehicle C on lane two at position x_C , it is under the shadowing of this big vehicle B if and only if $2x_B - L \leq x_C \leq D$ or equivalently $0 \leq x_B \leq (x_C + L)/2$. Hence, the probability that position x_C is not in the shadow region is given by

$$\begin{aligned} \Pr(\text{non-shadow}) &= \Pr\left(B = 0 \text{ within range } \frac{x_C + L}{2}\right) \\ &= e^{-\lambda_B \frac{x_C + L}{2}}. \end{aligned} \quad (55)$$

Then, the expected range of the shadowing region on lane two, caused by big vehicle on lane one, can be obtained by summing up all small dx_C from 0 to D , multiplied by the probability of being shadowed, i.e.,

$$\begin{aligned} SD_{112} &= \int_0^D \left(1 - e^{-\lambda_B \frac{x_C + L}{2}}\right) dx_C \\ &= D - \frac{2e^{-\frac{\lambda_B L}{2}}}{\lambda_B} \left(1 - e^{-\frac{\lambda_B D}{2}}\right). \end{aligned} \quad (56)$$

B. SD_{122} Formulation

The big vehicle B , located at position x_B on lane two, will cast the geometrical shadow region on lane two from point N to point P as shown in Fig. 12. Let us consider two equal right triangles OMN and NPQ . The position of point N is at $x_B + L/2$, while the position of point P is at $2(x_B + L/2)$. The geometrical shadow region on lane two is from $(x_B + L/2)$ to $(2x_B + L)$. A normal vehicle C on lane two at position x_C is shadowed if and only if $x_B + L/2 \leq x_C \leq 2x_B + L$. We split the region into two parts as follows.

Firstly, when $x_C \leq L$, the vehicle C is shadowed by B if $0 \leq x_B \leq x_C - L/2$. Then the probability that C is not in the

shadow region is given by

$$\begin{aligned} \Pr(\text{non-shadow}) &= \Pr\left(B = 0 \text{ within range } \left(x_C - \frac{L}{2}\right)\right) \\ &= e^{-\lambda_B(x_C - \frac{L}{2})}. \end{aligned} \quad (57)$$

Secondly, when $x_C > L$, the vehicle C is shadowed by B if $x_B + L/2 \leq x_C \leq 2x_B + L$ or equivalently, $(x_C - L)/2 \leq x_B \leq x_C - L/2$. The probability that C is not in the shadow region is given by

$$\begin{aligned} \Pr(\text{non-shadow}) &= \Pr\left(B = 0 \text{ within range } \frac{x_C}{2}\right) \\ &= e^{-\lambda_B \frac{x_C}{2}}. \end{aligned} \quad (58)$$

The expected range of shadowing region on lane two, caused by a big vehicle on lane two is

$$\begin{aligned} SD_{122} &= \int_{L/2}^L \left(1 - e^{-\lambda_B(x_C - \frac{L}{2})}\right) dx_C \\ &\quad + \int_L^D \left(1 - e^{-\lambda_B \frac{x_C}{2}}\right) dx_C \\ &= D + \frac{L}{2} + \frac{1}{\lambda_B} e^{-\frac{\lambda_B L}{2}} + \frac{2}{\lambda_B} e^{-\frac{\lambda_B D}{2}} - \frac{3}{\lambda_B}. \end{aligned} \quad (59)$$

ACKNOWLEDGMENT

Any opinions, findings and conclusions or recommendations expressed in this material are those of the author(s) and do not reflect the views of A*STAR.

REFERENCES

- [1] J. B. Kenney, "Dedicated short-range communications (DSRC) standards in the United States," *Proc. IEEE*, vol. 99, no. 7, pp. 1162–1182, Jul. 2011.
- [2] M. Noor-A-Rahim, G. G. M. N. Ali, Y. L. Guan, B. Ayalew, P. H. J. Chong, and D. Pesch, "Broadcast performance analysis and improvements of the LTE-V2V autonomous mode at road intersection," *IEEE Trans. Veh. Technol.*, vol. 68, no. 10, pp. 9359–9369, Oct. 2019.
- [3] H. Bagheri et al., "5G NR-V2X: Toward connected and cooperative autonomous driving," *IEEE Commun. Standards Mag.*, vol. 5, no. 1, pp. 48–54, Mar. 2021.
- [4] Y. P. Fallah, C. L. Huang, R. Sengupta, and H. Krishnan, "Analysis of information dissemination in vehicular ad-hoc networks with application to cooperative vehicle safety systems," *IEEE Trans. Veh. Technol.*, vol. 60, no. 1, pp. 233–247, Jan. 2011.
- [5] C. Han, M. Dianati, R. Tafazolli, R. Kernchen, and X. Shen, "Analytical study of the IEEE 802.11p MAC sublayer in vehicular networks," *IEEE Trans. Intell. Transp. Syst.*, vol. 13, no. 2, pp. 873–886, Jun. 2012.
- [6] Y. Yao, L. Rao, and X. Liu, "Performance and reliability analysis of IEEE 802.11p safety communication in a highway environment," *IEEE Trans. Veh. Technol.*, vol. 62, no. 9, pp. 4198–4212, Nov. 2013.
- [7] R. He, A. F. Molisch, F. Tufvesson, Z. Zhong, B. Ai, and T. Zhang, "Vehicle-to-vehicle propagation models with large vehicle obstructions," *IEEE Trans. Intell. Transp. Syst.*, vol. 15, no. 5, pp. 2237–2248, Oct. 2014.
- [8] T. Abbas, K. Sjöberg, J. Karedal, and F. Tufvesson, "A measurement based shadow fading model for vehicle-to-vehicle network simulations," *Int. J. Antennas Propag.*, vol. 2015, pp. 1–12, 2015.
- [9] M. G. Nilsson, D. Vlastaras, T. Abbas, B. Bergqvist, and F. Tufvesson, "On multilink shadowing effects in measured V2V channels on highway," in *Proc. 9th Eur. Conf. Antennas Propag.*, 2015, pp. 1–5.
- [10] R. Meireles, M. Boban, P. Steenkiste, O. Tonguz, and J. Barros, "Experimental study on the impact of vehicular obstructions in VANETs," in *Proc. IEEE Veh. Netw. Conf.*, 2010, pp. 338–345.
- [11] M. Boban, T. T. V. Vinhoza, M. Ferreira, J. Barros, and O. K. Tonguz, "Impact of vehicles as obstacles in vehicular ad hoc networks," *IEEE J. Sel. Areas Commun.*, vol. 29, no. 1, pp. 15–28, Jan. 2011.
- [12] M. Boban, X. Gong, and W. Xu, "Modeling the evolution of line-of-sight blockage for V2V channels," in *Proc. IEEE 84th Veh. Technol. Conf.*, 2016, pp. 1–7.
- [13] R. Huang, J. Wu, C. Long, Y. Zhu, B. Li, and Y. Lin, "Mitigate the obstructing effect of vehicles on the propagation of VANETs safety-related information," *IEEE Trans. Veh. Technol.*, vol. 67, no. 7, pp. 5558–5569, Jul. 2018.
- [14] M. Wang et al., "Comparison of LTE and DSRC-Based connectivity for intelligent transportation systems," in *Proc. IEEE Veh. Technol. Conf.*, 2017, pp. 1–5.
- [15] H. Nguyen et al., "Impact of big vehicle shadowing on vehicle-to-vehicle communications," *IEEE Trans. Veh. Technol.*, vol. 69, no. 7, pp. 6902–6915, Jul. 2020.
- [16] M. Boban, R. Meireles, J. Barros, P. Steenkiste, and O. K. Tonguz, "TVR-tall vehicle relaying in vehicular networks," *IEEE Trans. Mobile Comput.*, vol. 13, no. 5, pp. 1118–1131, May 2014.
- [17] G. G. M. N. Ali, M. Noor-A-Rahim, M. A. Rahman, S. K. Samantha, P. H. J. Chong, and Y. L. Guan, "Efficient real-time coding-assisted heterogeneous data access in vehicular networks," *IEEE Internet Things J.*, vol. 5, no. 5, pp. 3499–3512, Oct. 2018.
- [18] H. Nguyen, M. Noor-A-Rahim, Z. Liu, D. Jamaludin, and Y. Guan, "A semi-empirical performance study of two-hop DSRC message relaying at road intersections," *Information*, vol. 9, no. 6, Jun. 2018, Art. no. 147.
- [19] K. A. Hafeez, L. Zhao, B. Ma, and J. W. Mark, "Performance analysis and enhancement of the DSRC for VANET's safety applications," *IEEE Trans. Veh. Technol.*, vol. 62, no. 7, pp. 3069–3083, Sep. 2013.
- [20] K. A. Hafeez, A. Anpalagan, and L. Zhao, "Optimizing the control channel interval of the DSRC for vehicular safety applications," *IEEE Trans. Veh. Technol.*, vol. 65, no. 5, pp. 3377–3388, May 2016.
- [21] H. Peng et al., "Performance analysis of IEEE 802.11p DCF for multi-platooning communications with autonomous vehicles," *IEEE Trans. Veh. Technol.*, vol. 66, no. 3, pp. 2485–2498, Mar. 2017.
- [22] M. Haenggi, J. G. Andrews, F. Baccelli, O. Dousse, and M. Franceschetti, "Stochastic geometry and random graphs for the analysis and design of wireless networks," *IEEE J. Sel. Areas Commun.*, vol. 27, no. 7, pp. 1029–1046, Sep. 2009.
- [23] J. Teichmann, F. Ballani, and K. G. van den Boogaart, "Generalizations of Matn's hard-core point processes," *Spatial Statist.*, vol. 3, pp. 33–53, Feb. 2013.
- [24] G. Cecchini, A. Bazzi, B. M. Masini, and A. Zanella, "MAP-RP: Map-based resource reselection procedure for autonomous LTE-V2V," in *Proc. IEEE 28th Annu. Int. Symp. Pers., Indoor Mobile Radio Commun.*, 2018, pp. 1–6.
- [25] M. Gonzalez-Martín, M. Sepulcre, R. Molina-Masegosa, and J. Gozalvez, "Analytical models of the performance of C-V2X mode 4 vehicular communications," *IEEE Trans. Veh. Technol.*, vol. 68, no. 2, pp. 1155–1166, Feb. 2019.
- [26] A. Bazzi, B. M. Masini, A. Zanella, and I. Thibault, "On the performance of IEEE 802.11p and LTE-V2V for the cooperative awareness of connected vehicles," in *IEEE Trans. Veh. Technol.*, vol. 66, no. 11, pp. 10419–10432, Nov. 2017.
- [27] C. A. Balanis, *Antenna Theory: Analysis and Design*, 4th ed. Hoboken, NJ, USA: Wiley, 2016.
- [28] T. Abbas, A. Thiel, T. Zemen, C. F. Mecklenbrauker, and F. Tufvesson, "Validation of a non-line-of-sight path-loss model for V2V communications at street intersections," in *Proc. 13th Int. Conf. ITS Telecommun.*, 2013, pp. 198–203.
- [29] Cellular V2X Device-to-Device Communication, (CV2X) Consortium, "C-V2X performance assessment project," Dec. 2019. [Online]. Available: <https://pronto-core-cdn.prantomarketing.com/2/wpcontent/uploads/sites/2896/2020/02/CAMPVCV2XSAE01152020v2.pdf>



Hieu T. Nguyen received the Ph.D. degree in electronics engineering from Chungbuk National University, Cheongju, South Korea, in 2007. He is currently a Research Fellow with the School of Electrical and Electronic Engineering, Nanyang Technological University, Singapore. His main research interests include signal processing for communications, multicarrier and multiple-antenna systems, and vehicular communications.



Md. Noor-A-Rahim received the Ph.D. degree from the Institute for Telecommunications Research, University of South Australia, Adelaide, SA, Australia, in 2015. He was a Postdoctoral Research Fellow with the Centre for Infocomm Technology, Nanyang Technological University, Singapore. He is currently a Research Fellow with the School of Computer Science & IT, University College Cork, Ireland. His research interests include control over wireless networks, intelligent transportation systems, machine learning, signal processing, and DNA-based data storage. He was the recipient of the Michael Miller Medal from the Institute for Telecommunications Research, University of South Australia, for the most outstanding Ph.D. thesis in 2015.



Yong Liang Guan (Senior Member, IEEE) received the Ph.D. degree from Imperial College London, U.K., and the Bachelor of Engineering degree (with first class Hons.) from the National University of Singapore, Singapore. He is currently a Professor of communication engineering with the School of Electrical and Electronic Engineering, Nanyang Technological University (NTU), Singapore, where he leads the Continental-NTU Corporate Research Lab and led the successful deployment of the campus-wide NTU-NXP V2X Test Bed. He has authored or coauthored an invited monograph, more than books and more than 450 journal and conference papers. He has secured more than S\$70 million of external research funding. He has 15 filed patents and three granted patents, one of which was licensed to NXP Semiconductors. His research interests include coding and signal processing for communication systems and data storage systems. He is the Editor of IEEE TRANSACTIONS ON VEHICULAR TECHNOLOGY. He is also an Associate Vice President of NTU and a Distinguished Lecturer of the IEEE Vehicular Technology Society.



Dirk Pesch (Senior Member, IEEE) received the Dipl.Ing. degree from RWTH Aachen University, Aachen, Germany, and the Ph.D. degree from the University of Strathclyde, Glasgow, U.K. He is currently a Professor with the School of Computer Science and Information Technology, University College Cork and was the Head of the Nimbus Research Centre, Cork Institute of Technology (now Munster Technological University). He has more than 25 years research and development experience in both industry and academia and has authored or coauthored more than 200 scientific articles and book chapters. His research interests include architecture, design, algorithms, and performance evaluation of low power, dense and vehicular wireless/mobile networks and services for Internet of Things and Cyber-Physical System's applications in building management, smart connected communities, health and wellbeing, and smart manufacturing. He is a Principal Investigator of the National Science Foundation Ireland funded collaborative centres CONNECT (Future Networks) and CONFIRM (Smart Manufacturing), and the Director of the SFI Centre for Research Training in Advanced Networks for Sustainable Societies. He is also involved in a number of EU funded research projects on smart and energy efficient buildings and urban neighbourhoods, including as coordinator. Dirk contributes to international conference organization and is a Member of the Editorial Board of a number of journals.